Published in final edited form as:
Cancer Res. 2009 March 1; 69(5): 1951–1957. doi:10.1158/0008-5472.CAN-08-2023.

Chemoresistant Colorectal Cancer Cells, the Cancer Stem Cell Phenotype and Increased Sensitivity to Insulin-like Growth Factor Receptor-1 Inhibition

Nikolaos A. Dallas[1], **Ling Xia**[2], **Fan Fan**[2], **Michael J. Gray**[1], **Puja Gaur**[1], **George van Buren II**[1], **Shaija Samuel**[2], **Michael P. Kim**[1], **Sherry J. Lim**[1], and **Lee M. Ellis**[1,2]

[1]Department of Surgical Oncology, The University of Texas M. D. Anderson Cancer Center, Houston, Texas

[2]Department of Cancer Biology, The University of Texas M. D. Anderson Cancer Center, Houston, Texas

Abstract

5-fluorouracil (5FU) and oxaliplatin are standard therapy for metastatic colorectal cancer (CRC), but the development of chemoresistance is inevitable. Since cancer stem cells (CSCs) are hypothesized to be chemoresistant, we investigated CSC properties in newly developed chemoresistant CRC cell lines and sought to identify targets for therapy. The human CRC cell line HT29 was exposed to increasing doses of 5FU (HT29/5FU-R) or oxaliplatin (HT29/Ox) to achieve resistance at clinically relevant doses. Western blotting and flow cytometry were done to determine molecular alterations. The insulin-like growth factor 1 receptor (IGF-1R) monoclonal antibody (MoAb) AVE-1642 was used to inhibit signaling *in vitro* and *in vivo* using murine xenograft models. HT29/5FU-R and HT29/OxR demonstrated 16- to 30-fold enrichment of CD133+ cells and 2-fold enrichment of CD44+ cells (putative CRC CSC markers). Resistant cells were enriched 5- to 22-fold for double-positive (CD133+/CD44+) cells. Consistent with the CSC phenotype, resistant cells exhibited a decrease in cellular proliferation *in vitro* (47–59%; $p<0.05$). Phosphorylated and total IGF-1R levels were increased in resistant cell lines. HT29/5FU-R and HT29/OxR cells were ~5-fold more responsive to IGF-1R inhibition relative to parental cells ($p<0.01$) *in vitro*. Tumors derived from HT29/OxR cells demonstrated significantly greater growth inhibition in response to an IGF-1R MoAB than did parental cells ($p<0.05$).

Chemoresistant CRC cells are enriched for CSC markers and the CSC phenotype. Chemotherapy-induced IGF-1R activation provided for enhanced sensitivity to IGF-1R targeted therapy. Identification of CSC targets presents a novel therapeutic approach in this disease.

Introduction

Colorectal cancer (CRC) is the second leading cause of cancer death in the United States with about 50,000 deaths estimated for 2008 alone (1). Almost 25% of patients who present with colorectal cancer present with metastatic disease, and thousands of patients receive treatment for metastatic CRC each year (2). Significant improvements in patient survival rates have been achieved in recent years, largely due to the availability of targeted molecular therapies in addition to the standard chemotherapeutic regimens. The median overall survival duration for patients with metastatic CRC is currently about 20 months; however, most patients still die of their disease (3). While the response rate to current systemic

Correspondence: Lee M. Ellis, Department of Surgical Oncology, Unit 444, The University of Texas M. D. Anderson Cancer Center, P.O. Box 301402, Houston, TX 77230-1402, USA. Phone: 713-792-6926; Fax: 713-792-4689; lellis@mdanderson.org.

therapies is nearly 50%, resistance develops in nearly all patients. Therefore, it is essential to understand mechanisms of resistance as a first step in developing approaches to preventing or reversing chemoresistance in patients who receive systemic therapy for metastatic CRC.

5-Fluorouracil (5FU) and oxaliplatin are the mainstays of chemotherapeutic regimens for metastatic CRC. 5FU inhibits activity of the enzyme thymidylate synthase during DNA replication (4). In contrast, oxaliplatin covalently binds DNA, forming platinum-DNA adducts that cause prolonged G_2 arrest and inhibition of growth, which leads to apoptotic cell death (5). Although resistance mechanisms have been extensively studied for both of these agents, therapies to target resistance pathways have yet to be identified. There is an emerging body of evidence that tumor cells that are resistant to chemotherapy represent a subpopulation of cells from the original tumor that are molecularly and phenotypically distinct. These cells are referred to by several names, including tumor-initiating cells, tumor-promoting cells, or more commonly, cancer stem cells (CSCs) (6).

Experimental evidence for the existence of CSCs in CRC was recently demonstrated using human surgical specimens (7–9). Cells characterized by the expression or the absence of the transmembrane surface marker CD133 were isolated from fresh CRC tumors and injected into NOD-SCID mice. Tumors resulting from $CD133^+$ cells resembled the primary tumor from which they were derived and were more tumorigenic than were $CD133^-$ cells. Several other markers have been identified as putative CSC markers, including CD44, epithelial surface antigen, and CD166 (9). There is no consensus as to the exact criteria that define a CSC, as markers may vary according to tumor type. However, several functional studies have identified characteristics of these cells, including inherent chemoresistance, the ability to efflux Hoechst dye, the tendency to form spherical colonies *in vitro*, and the ability, in limited numbers, to form tumors in immunodeficient mice (reviewed in Tang et al (10)). Several other properties have been identified in organ-specific CSCs, and new studies are continuously being reported further characterizing the CSC phenotype.

Perhaps the most clinically relevant parameter of CSCs is their resistance to standard chemotherapeutic agents, and thus there is a great deal of interest in attempting to identify new targets for specifically eradicating these cells. Recent attention has been given to notch signaling (11), the sonic hedgehog pathway (12, 13), and growth factor receptors.

Given the clinical significance of chemoresistance and the ineffectiveness of chemotherapy in eliminating CSCs, we chose to evaluate the relationship between chemoresistance and the CSC phenotype. We developed two chemoresistant cell lines from a chemosensitive parental human CRC cell line and investigated their molecular and phenotypic alterations *in vitro* and *in vivo*. After we detected activation of the insulin-like growth factor 1 receptor (IGF-1R) pathway in the chemoresistant cell lines, we targeted this pathway in several xenograft studies.

Materials and Methods

Cell lines and culture conditions

The human CRC cell line HT29 was obtained from the American Type Culture Collection (Manassas, VA). The oxaliplatin-resistant cell line, HT29/OxR, was developed in our laboratory as previously described (14). Cells stably resistant to 5FU were developed by exposing parental HT29 cells to an initial dose of 0.1 μg/ml and culturing surviving cells to a confluence of 80% for three passages (~6 weeks). The cells that survived initial 5FU treatment were then exposed to 0.5 μg/ml 5FU for three passages (~8 weeks), then 1.0 μg/ml for 3 passages (~8 weeks). Finally, the 5FU concentration was increased to the clinically

relevant plasma concentration of 2 μg/ml for 3 weeks (10 weeks). The surviving resistant cells were named HT29/5FU-R.

All cells were cultured in minimum essential medium (MEM) supplemented with 10% fetal bovine serum (FBS), vitamins, nonessential amino acids, penicillin-streptomycin, sodium pyruvate, and L-glutamine (Life Technologies, Grand Island, NY). Oxaliplatin- and 5FU-resistant cells were continuously cultured in 2 μmol/L and 2 μg/ml of the respective drugs, unless otherwise indicated. *In vitro* experiments were carried out at 70% cell confluence and confirmed in at least three independent experiments.

Drugs and antibodies

Oxaliplatin and 5FU were purchased from the M. D. Anderson Cancer Center pharmacy. The monoclonal antibody (MoAb) AVE-1642 (provided by sanofi-aventis, Bridgewater, NJ) was used to inhibit IGF-1R signaling *in vitro* and *in vivo* and has been previously described (15). Antibodies used for flow cytometry, immunohistochemical analysis, immunofluorescence, or Western blotting were as follow: rabbit anti-CD133, rabbit anti-phosphorylated-IGF-1R, (Cell Signaling Technology, Danvers, MA), mouse anti-vinculin, rabbit anti-β-actin (Sigma-Aldrich, St. Louis, MO), mouse anti-CD44 (Abcam, Cambridge, UK), phycoerythrin (PE)-conjugated anti-CD133, PE-conjugated mouse-IgG1 (Miltenyi Biotec, Auburn, CA), flurorescein isothiocyanate (FITC)-conjugated anti-CD44, FITC-conjugated mouse-IgG2b, rabbit anti-IGF-1R (Santa Cruz Biotechnology, Santa Cruz, CA), and mouse anti-Ki67 (Dako, Carpinteria, CA).

Western blotting

For all Western blot analyses, protein was harvested from cells plated to 70–80% confluence. Whole-cell lysates were isolated using radioimmunoprecipitation assay B protein lysis buffer as previously described (16). Secreted proteins were obtained from conditioned media after cells were plated in 1% FBS medium for 48 hours; medium was harvested and concentrated using Amicon Ultra Centrifugal Filter Devices (Millipore Corp., Billerica, MA). Quantification of these proteins was completed using a modified Bradford assay (Bio-Rad Laboratories, Hercules, CA). Protein samples for Western blotting were prepared by boiling after the addition of denaturing sample buffer. Proteins were separated using sodium dodecyl sulfate polyacrylamide gel electrophoresis (SDS-PAGE) on an 8% or 15% gel and transferred to a polyvinylidene difluoride membrane (Millipore Corp., Billerica, MA) by electroblotting. Antibodies were diluted in TBS and 0.1% (v/v) Tween with 5% nonfat dry milk after 1 hour of protein blocking in the absence of antibody. Membranes were incubated at 4°C overnight with primary antibody. Membranes were subsequently washed and incubated with the appropriate horseradish peroxidase–conjugated secondary antibody (Amersham Biosciences, Piscataway, NJ) for 1 hour at room temperature. Membranes were again washed, and protein bands were visualized using a commercially available enhanced chemiluminescence kit (Amersham Biosciences). When appropriate, membranes were incubated in stripping solution for 30 minutes at 65°C, washed, and reprobed with a second primary antibody for verification of loading control.

Flow cytometry and cell cycle analysis

Cells were prepared for analysis of cell surface marker expression by plating to 70% confluence the day prior to analysis. Cells were then detached from plates by incubation with enzyme-free cell dissociation buffer (Invitrogen, Carlsbad, CA). Cells were washed in phosphate-buffered saline and resuspended in 1% bovine serum albumin plus fluorophore-conjugated primary antibodies for 30 minutes at room temperature. Samples were then washed and analyzed using a Cell Lab Quanta^{TM} flow cytometer coupled to a computer with data acquisition and analysis software (Beckman Coulter, Fullerton, CA).

Proliferation and chemosensitivity assay

Rates of proliferation and sensitivity to drugs were assessed using the colorimetric 3-(4,5-dimethylthiazol-2-yl)-2,5-diphenyltetrazolium bromide (MTT) assay as described previously (17). Briefly, 2,500 cells of each cell line were plated per well in 96-well plates in 200 μl medium with or without drug (5FU, oxaliplatin, AVE-1642). At each time point (0 h, 24 h, 48 h, and 72 h), 40 μl MTT solution was added to each well and the plate was incubated for 1 hr at 37°C. Medium was then aspirated from each well, and 100 μl of dimethyl sulfoxide was added. Colorimetric analysis was performed at a wavelength of 570 nm using a standard microplate reader. Doubling times were calculated by plotting growth curves on Excel v2003.SP2 software (Microsoft Corporation, Redmond, WA) and using the built-in exponential regression algorithm.

Colonosphere assay

The ability of cell lines to form spheres in suspension was evaluated as described by Liu et al., with modifications (13). Dulbecco's modified Eagle medium (DMEM) with B27 supplement (Gibco, Carlsbad, CA), 20 μg/ml epidermal growth factor (Invitrogen), 20 μg/ml fibroblast growth factor (Invitrogen), and penicillin-streptomycin served as the stem cell medium (SCM) for these experiments. An equal number of cells from parental HT29 cells and each chemoresistant cell line were plated at a concentration of 200 cells/100 μl SCM in each of 32 wells of a 96-well ultra-low-attachment plate (Corning Life Sciences, Lowell, MA). Cells were supplemented with 100 μl SCM after 5 days of incubation and analyzed on day 10, when the formation of colonospheres was evaluated by light microscopy. In order to quantitate the difference in numbers of spheres between cell lines, MTT solution (40 μl) was added to each well, and colorimetric assessment was conducted as above. The average optical density measurements for each cell line from 32 wells was used as an index of sphere number.

Anchorage-independent growth assay

Soft agar assays were used to determine the ability of parental and chemoresistant cell lines to grow under anchorage-independent conditions. Each well of a 6-well plate was coated with 1 ml of 10% FBS medium with 1% agarose. After 20 minutes of incubation at 37°C, cell suspensions of an equal number (500) of parental and chemoresistant cells were added in 1 ml of medium with 0.5% agarose. Cells were incubated for 14 days under standard conditions (37°C, 5% CO_2) and with the addition of 300 μl of medium every 3 days to hydrate the exposed agarose. At the end of the incubation period, wells were examined under a light microscope at 20× magnification and the number of colonies larger than 50 μm were counted per well.

Subcutaneous xenograft model and IGF-1R inhibition

Male athymic nude mice, 6–8 weeks old, were obtained from the National Cancer Institute-Frederick Cancer Research Facility (Frederick, MD) and acclimated for 2 weeks. All animal studies were conducted under approved guidelines of the Animal Care and Use Committee of MDACC. Equal numbers of cells (10^6) from parental and chemoresistant cell lines were suspended in 100 μl phosphate-buffered saline and injected subcutaneously into the right rear flank of each mouse (20 mice per group). When tumors reached ~100 mm^3, intraperitoneal treatment with 1 mg/mouse AVE-1642 was initiated at a dosing frequency of twice per week for 10 mice in each group. Tumor growth was observed and recorded over 10 weeks. When tumors in the control group exceeded 1.5 cm in longest diameter, mice were killed by CO_2 asphyxiation according to protocol, and tumors were excised. Tumors were weighed and measured, and a portion of each was placed in 10% formalin (for paraffin

embedding), placed in optimal cutting temperature (OCT) compound, and snap-frozen in liquid nitrogen. Tumor volume was calculated as (length)/2 × (width)^2.

Immunohistochemistry and immunofluorescent analysis

Tumors preserved in formalin were placed in paraffin blocks and sectioned onto positively charged microscope slides. They were deparaffinized in xylene, hydrated in graded alcohol, and pretreated for antigen retrieval in citrate buffer for 20 minutes in a 98°C steamer. Tumor sections embedded in OCT compound were sectioned onto positively charged microscope slides and serially immersed in acetone, acetone:chloroform mixture (1:1), then acetone. Slides were then stained for hematoxylin and eosin to assess morphology, or anti-Ki67 antibodies to visualize proliferative nuclei. All immunohistochemical sections were counterstained with Gill No. 3 hematoxylin (Sigma-Aldrich). The DeadEnd^{TM} Fluorometric TUNEL System (Promega, Madison, WI) was used to identify and quantitate apoptotic cells in *in vivo* sections. Immunofluorescent slides were examined using a Nikon Microphot FXA fluorescent microscope, and representative images were obtained. Terminal deoxynucleotidyl transferase-mediated biotin-dUTP nick end labeling (TUNEL) images were processed using NIH ImageJ v1.34 software, converting TUNEL fluorescent images to binary images in order to quantitate staining. Immunohistochemical staining and fluorescence were quantitated using commercially available image analysis software (Photoshop v7.0, Adobe Systems Inc., San Jose, CA).

Results

Effect of chemoresistance on expression of CSC markers

The expression profiles of parental HT29 human CRC cells and cells resistant to 5FU or oxaliplatin (HT29/5FU-R or HT29/OxR, respectively) were evaluated by Western blot and flow cytometric analyses. HT29/5FU-R and HT29/OxR cells expressed significantly more CD133 and CD44, putative CSC markers (7, 8), than did parental HT29 cells (Figure 1A). The number of cells that expressed CD133 and CD44 was also significantly greater in the chemoresistant cell lines than in parental cells (Figure 1B). Whereas only 2% of parental cells expressed CD133 and 43% expressed CD44, more than 36% of HT29/5FU-R and 57% of HT29/OxR cells expressed CD133, and 95% of both types of chemoresistant cells expressed CD44. In fact, 5FU-resistant cells were ~5-fold and oxaliplatin-resistant cells ~22-fold enriched for cells positive for both CD133 and CD44 (Figure 1C).

Effect of chemoresistance on the cellular phenotype

In vitro proliferation was assessed by plating equal numbers of cells of each cell line and by using MTT assay as an index of cell number. The proliferation rates of both 5FU- and oxaliplatin-resistant cells were significantly lower than that of the parental cells ($p<0.05$; Figure 2A). Specifically, the doubling time of parental HT29 cells was 17 hrs, whereas the doubling times of HT29/5FU-R and HT29/OxR cells were 32 hours and 42 hours ($p<0.05$ vs. parental cells), respectively. MTT assay was also used to evaluate sensitivity to chemotherapeutic agents. Parental and 5FU- and oxaliplatin-resistant cells were exposed to clinically relevant doses of 5FU and oxaliplatin, and the remaining number of cells was evaluated after 48 hours. Parental cells were sensitive to both oxaliplatin and 5FU, with only 40% and 58% of viable cells remaining after exposure to drug, respectively (Figure 2B). 5FU-resistant cells were resistant to 5FU as expected, but these cells were also resistant to oxaliplatin, with 80% of viable cells remaining after 72 hours of exposure. Similarly, oxaliplatin-resistant cells were resistant to oxaliplatin as expected, but also showed cross-resistance to 5FU.

CSCs have the described ability to form colonies, or spheres, in the absence of serum and without attachment to culture plates (13). We evaluated the ability of parental and chemoresistant cell lines to grow colon cancer cell spheres, or colonospheres, under serum-free conditions. Differences between cell lines were quantitated by plating a limited number of cells in each well of a low-attachment 96-well plate and evaluating the ability of cells to form colonospheres. HT29/5FU-R and HT29/OxR cells had an increased number of spheres relative to parental cells ($p<0.05$; Figure 2C). Chemoresistant cells also demonstrated an increased ability to form colonies under anchorage-independent conditions in a standard soft-agar assay after 14 days in culture (Figure 2D).

Effect of chemoresistance on IGF-1R signaling

Constitutive signaling in parental and chemoresistant cell lines, with a focus on targets for which agents that inhibit target function are readily available, was evaluated by Western blotting. We studied the activation status of several growth factor receptors but focused our efforts on IGF-IR, for which we observed the most marked alterations. Levels of phosphorylated IGF-1R were higher in both HT29/5FU-R and HT29/OxR cells than in parental cells (Figure 3A). Levels of total IGF-1R were also increased in the chemoresistant cell lines.

The IGF-1R MoAb AVE-1642 was used to determine the cells' dependence on IGF-1R signaling for survival. MTT assay demonstrated that AVE-1642 treatment of chemoresistant cells led to only a minor decrease (13%) in cell number in the parental cells but a significantly greater reduction in cell number in the chemoresistant cells relative to the parental cells (48% for HT29/5FU-R and 54% for HT29/OxR; $p<0.05$ in each case; Figure 3B).

We further evaluated whether treatment with AVE-1642 would restore chemosensitivity in our chemoresistant cell lines. Using the MTT assay, there were no differences between cells treated with AVE-1642 and those treated with both AVE-1642 and either 5FU or Ox after 48 hours of exposure (data not shown). This chemosensitivity assay was performed with both HT29/5FU-R and HT29/OxR cells, yielding similar results.

Effect of IGF-1R inhibition on *in vivo* tumor growth

Parental and chemoresistant cells were injected subcutaneously in the right flanks of nude mice, and tumor growth was assessed during biweekly treatment with AVE-1642 or with nonspecific, isotype-matched control MoAb. After ~4 weeks (at which time maximum tumor size approached 1.5 cm^3), tumors were harvested and analyzed. Tumors derived from parental and chemoresistant cells that were treated with AVE1642 were significantly smaller than those treated with control antibody (Figure 4A–B). However, HT29/5FU-R tumors and HT29/OxR tumors showed significantly greater tumor growth inhibition with AVE-1642 treatment than did parental cells. 5FU-resistant cells demonstrated 48% growth inhibition and oxaliplatin-resistant cells 65% growth inhibition relative to parental cells (17%; $p<0.05$).

Evaluation of a proliferative marker (Ki67) by staining of tumor sections demonstrated that the MoAb to IGF-1R led to a decrease in the number of proliferating cells in all tumors compared with those treated with control antibody. However, similar to tumor growth inhibition, blockade of IGF-1R led to a greater effect in chemoresistant tumors than in tumors from parental cells, although this difference did not reach statistical significance. TUNEL staining was used to evaluate apoptosis in xenografts. Quantification of TUNEL staining demonstrated that AVE-1642 treatment caused significantly more apoptosis in tumors derived from HT29/5FU-R and HT29/OxR cells than in tumors derived from HT29 cells ($p<0.05$; Figure 4C–D). Specifically, HT29 tumors demonstrated a 2.7-fold increase in

apoptotic nuclei with IGF-1R inhibition, compared with a 5.3-fold increase in HT29/5FU-R- and a 5.5-fold increase in HT29/OxR-derived tumors ($p<0.05$ in each case). Representative images from all tumor sections analyzed, in addition to photographs of subcutaneous tumors, can be seen in Figure 5.

Discussion

CRC is the second leading cause of cancer death in the United States. Despite recent therapeutic regimens that have significantly increased survival in metastatic disease, invariably, nearly all tumors become chemoresistant. Understanding the mechanisms of resistance in CRC is essential to optimizing current therapeutic strategies.

To address the issue of identifying potential targets in chemoresistant cell lines, we created two chemoresistant cell lines from the parental human CRC cell line HT29. HT29/5FU-R cells and HT29/OxR cells were developed to be resistant to 5FU and oxaliplatin, respectively, at the clinically relevant plasma concentrations of patients receiving these drugs. The oxaliplatin-resistant cell line was characterized in a previous study from our laboratory whereby oxaliplatin-resistant cells were shown to undergo epithelial-to-mesenchymal transition (EMT) (14). EMT-consistent changes were likewise observed in the HT29/5FU-resistant cell line (data not shown). In attempting to determine the mechanisms that imparted chemoresistance on our cell lines, we investigated these cells for CRC stem cell markers since CSCs are characterized by being chemoresistant.

Many investigators have used fluorescence-activated cell sorting to identify and isolate CSCs and determined that these cells are chemoresistant. We took the opposite approach by developing chemoresistant cells and then determining whether these cells acquired CSC characteristics. We determined that both 5FU- and oxaliplatin-resistant cells were significantly enriched for the CSC markers CD133 and CD44. Chemoresistant cells were also more quiescent *in vitro*, demonstrating a decrease in cellular proliferation relative to parental cells. However, HT29/5FU-R and HT29/OxR cells demonstrated an increased ability to form colonies in soft agar under anchorage-independent conditions and an increased ability to form spheres in specialized serum-free media, all properties consistent with the CSC phenotype (13, 18–20). Oxaliplatin-resistant cells demonstrated an increase in resistance to 5FU, and likewise, 5FU-resistant cells were cross-resistant to oxaliplatin. This finding suggests that acquired resistance to one chemotherapeutic agent activates general resistance pathways that impart resistance to multiple agents. Chemoresistant cells demonstrate enrichment of CSC markers and properties consistent with the CSC phenotype; however, definitive evidence that these cells are true CSCs has yet to be obtained, and alternate explanations for our findings do exist. For example, it is certainly plausible that the process of developing chemoresistant cell lines may incude increased expression of CSC markers rather than enrich for those cells already expressing these markers. Testing this hypothesis would be difficult, however, as little is known about the pathways involved and the expression pattern of CD133 in epithelial malignancies. In addition, studies in our laboratory have demonstrated that CSC marker expression is elevated in lysates obtained from cell line-derived CRC spheres relative to adherent tumor cells (data not shown). Given this finding and the data presented in this study, we have demonstrated two mechanisms by which selection of cells using either sphere formation or chemoresistance enriches for CSC marker expressing cells. To definitively explain our findings, further studies to elucidate the mechanism of resistance and increased marker expression are needed.

We also investigated the activation status of growth factor receptors in response to chemoresistance in a focused attempt to identify potential mediators in the chemoresistant cells that would allow specific targeting of these cells with available agents. One such

pathway was the IGF-1R signaling pathway, known to be involved in CRC progression and growth (21, 22). In this study, constitutive IGF-1R levels were greater in chemoresistant cell lines relative to parental cell lines, more notably in the oxaliplatin-resistant line. The increase in IGF-1R phosphorylation is associated with the increase of total levels of the receptor. The attribution of the increase in IGF-1R phosphorylation being due to an increase in total levels of IGF-1R is supported by the fact that there were no demonstrable changes in expression of the ligands for IGF-1R (IGF-1 and IGF-2) (data not shown). The precise mechanism of the increase in IGF-1R expression in these cells remains unknown. Inhibition of Src and Akt signaling failed to block the increase in IGF-1R expression, ruling out these pathways as the mechanism for IGF-1R induction in chemoresistant cell lines.

Inhibition of IGF-1R *in vitro* led to a decrease in cell growth as determined by MTT assay, and these effects were greater in the chemoresistant cell lines. *In vivo*, after treatment with AVE-1642, inhibition of growth of tumors derived from 5FU- and oxaliplatin-resistant cells was significantly higher than the growth inhibition noted in tumors derived from parental cells. Our laboratory previously demonstrated that IGF-1R inhibition in an orthotopic model of metastatic colon cancer in the murine liver leads to decreased tumor growth by induction of tumor cell apoptosis (23). In this study, we demonstrated that IGF-1R inhibition caused a modest decrease in the growth of parental tumors (17% inhibition), whereas the effect on growth of chemoresistant cell-derived tumors was significantly greater (48% for HT29/5FU-R and 65% for HT29/OxR; $p<0.05$), which was largely due to an increase in apoptosis. Inhibition of IGF-1R *in vitro* did not lead to increased sensitivity to 5-FU or oxaliplatin, and thus *in vivo* studies using both AVE-1642 and 5FU or oxaliplatin were not performed.

In addition to IGF-1R, we studied several other growth factor receptors in the chemoresistant cell lines including epidermal growth factor receptor (EGFR), cMET, and RON (data not shown). However, we focused our studies in IGF-IR since preliminary studies *in vitro* utilizing inhibitors of each of the above mentioned pathways did not demonstrate significant effects on chemoresistant cell proliferation.

5FU and oxaliplatin act by distinct mechanisms to cause tumor cell cytotoxicity, and it is unlikely that acquired chemoresistance to these agents would yield common molecular alterations. However, our data show that when cells are chronically exposed to either agent, the resulting cells acquire similar molecular alterations that are characteristic of the CSC phenotype. Interestingly, these resistant cells expressed increased levels of IGF-IR (and, in turn, phosphorylated IGF-1R), making these cells more sensitive to blockade of this pathway. Recent data have suggested that the targeting of growth factor receptors such as that encoded by the *MET* proto-oncogene may be an effective method for targeting chemoresistant CSCs (reviewed in Boccaccio et al (24)). Similar to the activity of MET-kinase, our data suggest that IGF-1R inhibition may also target these cells. Our data lead us to further hypothesize that inhibition of IGF-1R signaling in the chemoresistant setting may be more effective than inhibition of this pathway in the front-line setting. This hypothesis requires further study in preclinical and clinical trials. IGF-1R inhibition may prove to be the therapeutic strategy that is effective in patients with otherwise untreatable disease.

Acknowledgments

We thank Sunita C. Patterson (Department of Scientific Publications) for manuscript editing and Rita Hernandez for editorial assistance.

Financial support: This work was supported by NIH-5 T32 CA09599 (NAD, MPK, GVB, PG, SJL), the R.E. “Bob” Smith Fund for Cancer Research (SS), The William C. Liedtke, Jr, Fund for Cancer Research (LME), NIH RO1 CA112390 (LME), and Sanofi-Aventis (LME).

References

1. Jemal A, Siegel R, Ward E, et al. Cancer statistics, 2008. CA Cancer J Clin. 2008; 58(2):71–96. [PubMed: 18287387]
2. Goldberg RM, Rothenberg ML, Van Cutsem E, et al. The continuum of care: a paradigm for the management of metastatic colorectal cancer. Oncologist. 2007; 12(1):38–50. [PubMed: 17227899]
3. Hurwitz H, Fehrenbacher L, Novotny W, et al. Bevacizumab plus irinotecan, fluorouracil, and leucovorin for metastatic colorectal cancer. N Engl J Med. 2004; 350(23):2335–2342. [PubMed: 15175435]
4. Walko CM, Lindley C. Capecitabine: a review. Clin Ther. 2005; 27(1):23–44. [PubMed: 15763604]
5. Kelland L. The resurgence of platinum-based cancer chemotherapy. Nat Rev Cancer. 2007; 7(8): 573–584. [PubMed: 17625587]
6. Reya T, Morrison SJ, Clarke MF, Weissman IL. Stem cells, cancer, and cancer stem cells. Nature. 2001; 414(6859):105–111. [PubMed: 11689955]
7. O'Brien CA, Pollett A, Gallinger S, Dick JE. A human colon cancer cell capable of initiating tumour growth in immunodeficient mice. Nature. 2007; 445(7123):106–110. [PubMed: 17122772]
8. Ricci-Vitiani L, Lombardi DG, Pilozzi E, et al. Identification and expansion of human colon-cancer-initiating cells. Nature. 2007; 445(7123):111–115. [PubMed: 17122771]
9. Dalerba P, Dylla SJ, Park IK, et al. Phenotypic characterization of human colorectal cancer stem cells. Proc Natl Acad Sci U S A. 2007; 104(24):10158–10163. [PubMed: 17548814]
10. Tang C, Ang BT, Pervaiz S. Cancer stem cell: target for anti-cancer therapy. Faseb J. 2007; 21(14): 3777–3785. [PubMed: 17625071]
11. Zhang XP, Zheng G, Zou L, et al. Notch activation promotes cell proliferation and the formation of neural stem cell-like colonies in human glioma cells. Mol Cell Biochem. 2008; 307(1–2):101–108. [PubMed: 17849174]
12. Tung DC, Chao KS. Targeting hedgehog in cancer stem cells: how a paradigm shift can improve treatment response. Future Oncol. 2007; 3(5):569–574. [PubMed: 17927522]
13. Liu S, Dontu G, Mantle ID, et al. Hedgehog signaling and Bmi-1 regulate self-renewal of normal and malignant human mammary stem cells. Cancer Res. 2006; 66(12):6063–6071. [PubMed: 16778178]
14. Yang AD, Fan F, Camp ER, et al. Chronic oxaliplatin resistance induces epithelial-to-mesenchymal transition in colorectal cancer cell lines. Clin Cancer Res. 2006; 12(14 Pt 1):4147–4153. [PubMed: 16857785]
15. Maloney EK, McLaughlin JL, Dagdigian NE, et al. An anti-insulin-like growth factor I receptor antibody that is a potent inhibitor of cancer cell proliferation. Cancer Res. 2003; 63(16):5073–5083. [PubMed: 12941837]
16. Jung YD, Liu W, Reinmuth N, et al. Vascular endothelial growth factor is upregulated by interleukin-1 beta in human vascular smooth muscle cells via the P38 mitogen-activated protein kinase pathway. Angiogenesis. 2001; 4(2):155–162. [PubMed: 11806247]
17. Gray MJ, Van Buren G, Dallas NA, et al. Therapeutic targeting of neuropilin-2 on colorectal carcinoma cells implanted in the murine liver. J Natl Cancer Inst. 2008; 100(2):109–120. [PubMed: 18182619]
18. Phillips TM, Kim K, Vlashi E, McBride WH, Pajonk F. Effects of recombinant erythropoietin on breast cancer-initiating cells. Neoplasia. 2007; 9(12):1122–1129. [PubMed: 18084619]
19. Todaro M, Alea MP, Di Stefano AB, et al. Colon cancer stem cells dictate tumor growth and resist cell death by production of interleukin-4. Cell Stem Cell. 2007; 1(4):389–402. [PubMed: 18371377]
20. Yu SC, Ping YF, Yi L, et al. Isolation and characterization of cancer stem cells from a human glioblastoma cell line U87. Cancer Lett. 2008
21. Reinmuth N, Fan F, Liu W, et al. Impact of insulin-like growth factor receptor-I function on angiogenesis, growth, and metastasis of colon cancer. Lab Invest. 2002; 82(10):1377–1389. [PubMed: 12379772]

22. Reinmuth N, Liu W, Fan F, et al. Blockade of insulin-like growth factor I receptor function inhibits growth and angiogenesis of colon cancer. Clin Cancer Res. 2002; 8(10):3259–3269. [PubMed: 12374697]

23. Bauer TW, Fan F, Liu W, et al. Targeting of insulin-like growth factor-I receptor with a monoclonal antibody inhibits growth of hepatic metastases from human colon carcinoma in mice. Ann Surg Oncol. 2007; 14(10):2838–2846. [PubMed: 17653802]

24. Boccaccio C, Comoglio PM. Invasive growth: a MET-driven genetic programme for cancer and stem cells. Nat Rev Cancer. 2006; 6(8):637–645. [PubMed: 16862193]

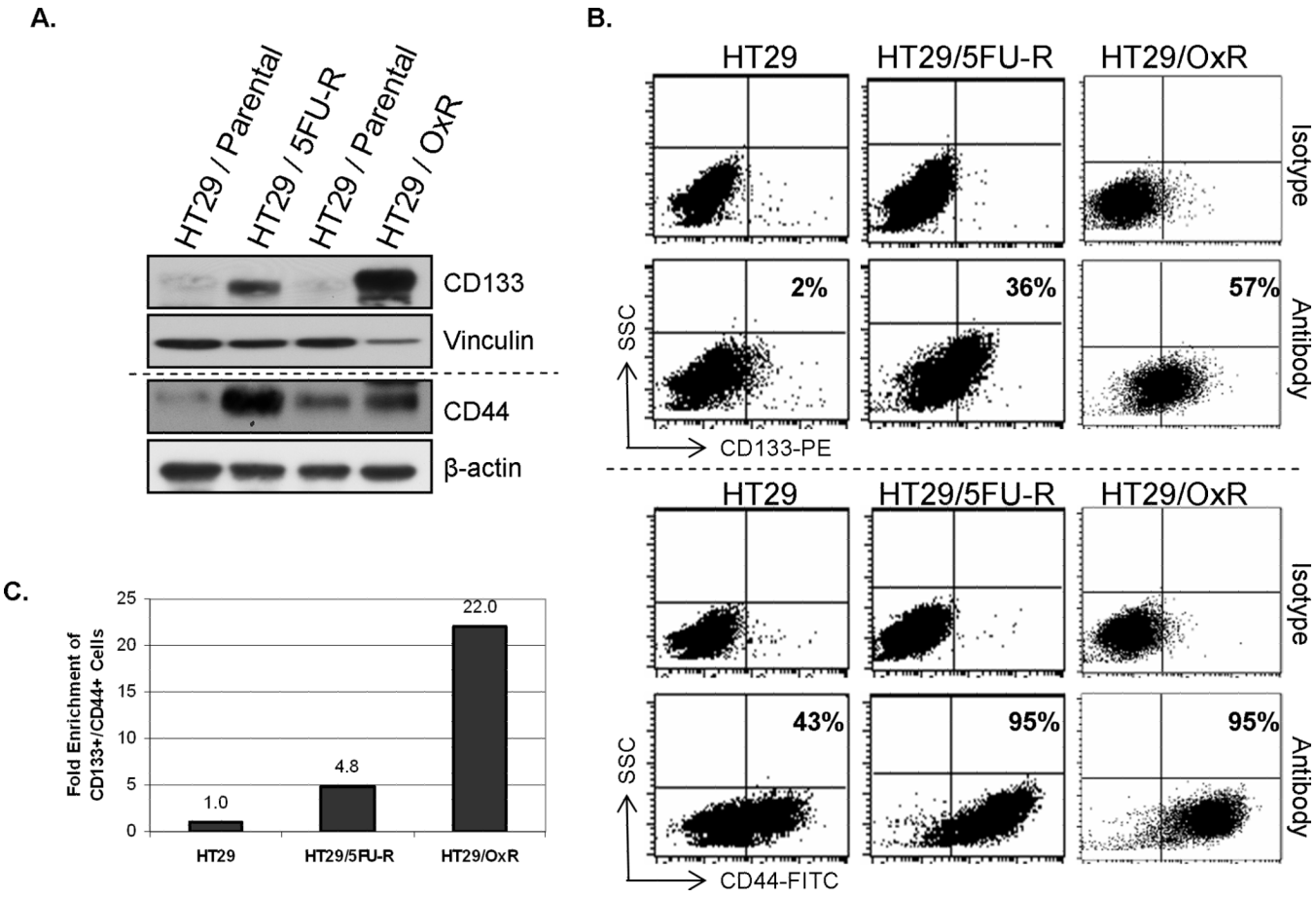

Figure 1. Chemoresistant cell lines are enriched for tumor stem cell markers

(A) Western blotting demonstrated that expression of the CRC stem cell markers CD133 and CD44 was higher in the chemoresistant cell lines HT29/5FU-R and HT29/OxR than in the parental HT29 human CRC cell line. Vinculin and β-actin levels are provided as loading controls (B) Flow cytometric analysis demonstrated that both chemoresistant cell lines were enriched for cells that expressed CD133 and CD44 when compared with the parental cell line. 36% of HT29/5FU-R cells and 57% of HT29/OxR cells expressed CD133 relative to 2% of HT29 cells. Similarly, 95% of chemo-resistant cells expressed CD44 relative to only 43% of parental cells. Cytometric analysis plots using isotype control antibodies are provided as staining controls. (C) When cells were labeled with both markers, flow cytometric analysis demonstrated ~5-fold enrichment of double-positive cells in the HT29/5FU-R cell line and ~22-fold enrichment in the oxaliplatinresistant cell line compared with the parental HT29 cell line. SCC = Side scatter.

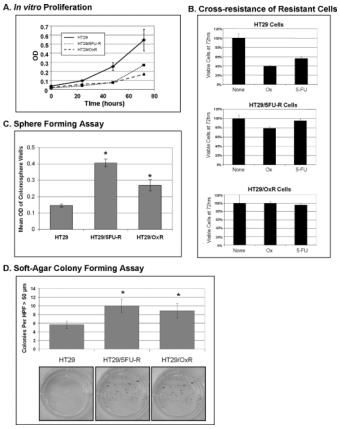

Figure 2. Chemoresistant cell lines are enriched for tumor stem cell phenotype

(A) Chemoresistant cells proliferate at a significantly slower rate than do parental cells by MTT analysis. (B) Parental cells demonstrate sensitivity to both 5FU and oxaliplatin after exposure to drug for 72 hours, with only 40% and 58% of cells remaining, respectively, relative to untreated cells. In contrast, HT29/5FU-R cells are resistant to 5FU as expected; however, they also demonstrate an increase in resistance to oxaliplatin relative to parental cells. Similarly, oxaliplatin-resistant cells are resistant to oxaliplatin but also are resistant to 5FU. (C) Cells were plated in an ultra-low-attachment 96-well plate in the absence of serum, and 14 days later the number of viable sphere-forming cells was assayed by MTT. Chemoresistant cells demonstrated a 2- to 3-fold increase in colonosphere-forming cells relative to parental cells. (D) In a soft agar assay, 5FU- and oxaliplatin-resistant cells formed significantly more colonies larger than 50 μm in diameter under anchorage-independent growth conditions when compared to HT29 cells. These findings are consistent with the described CSC phenotype. Error bars represent standard error of the mean, and asterisks denote $p<0.05$. HPF=High Power Field. OD = optical density.

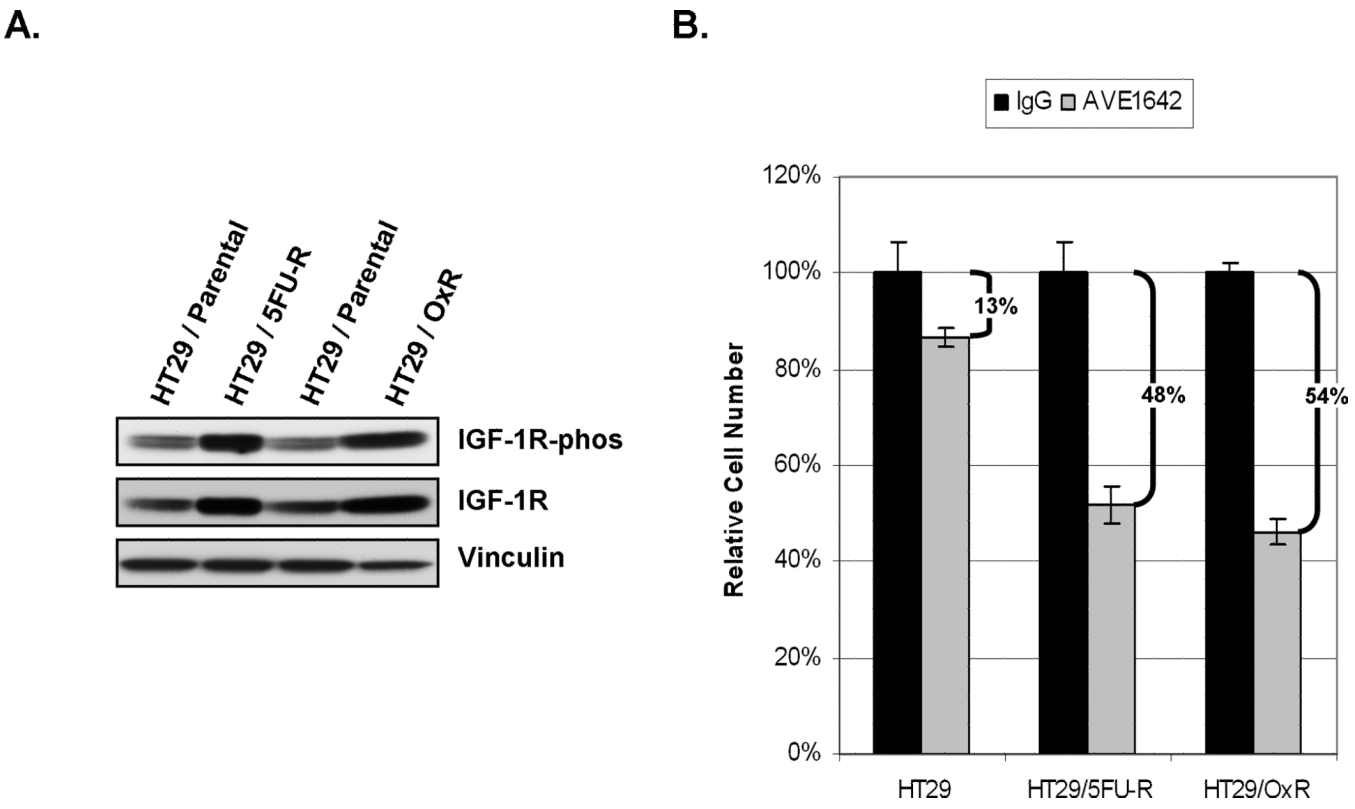

Figure 3. Effect of IGF-1R inhibition on chemoresistant cells

(A) Analysis of whole cell lysates from parental and resistant cells demonstrated an increase in both phosphorylation and total levels of IGF-1R in chemoresistant cells relative to parental cells. (B) Cells were treated with control or IGF-1R targeting antibodies, and the cell number relative to that of the control treatment was analyzed. There was a significantly greater decrease in cell number in the chemoresistant cells treated with AVE-1642 than in the parental cells (48%-54% vs. 13%; $p<0.05$).

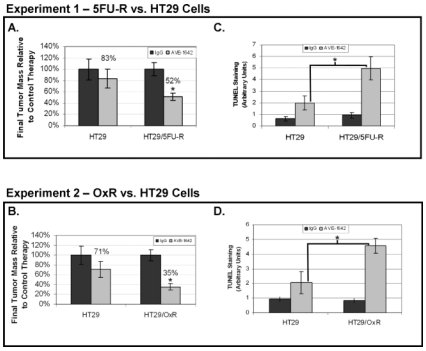

Figure 4. Effect of IGF-1R inhibition on *in vivo* tumor growth, proliferation, and apoptosis

Mice were subcutaneously injected with 1×10^6 HT29 or HT29/5FU-R cells in one experiment or HT29 or HT29/OxR cells in a second and treated with control IgG or AVE1642 twice weekly. The final tumor masses were measured and compared between mice bearing tumors from each cell line. Relative to control-treated mice, HT29/5FU-R-(A) and HT29/OxR-derived tumors (B) showed significantly greater growth inhibition than did HT29-derived tumors. TUNEL staining revealed significantly greater apoptosis in response to AVE1642 in tumors derived from HT29/5FU-R- (C) and HT29/OxRd-erived tumors (D) than in tumors derived from parental cells. Asterisks denote $p<0.05$ and error bars represent standard error of the mean.

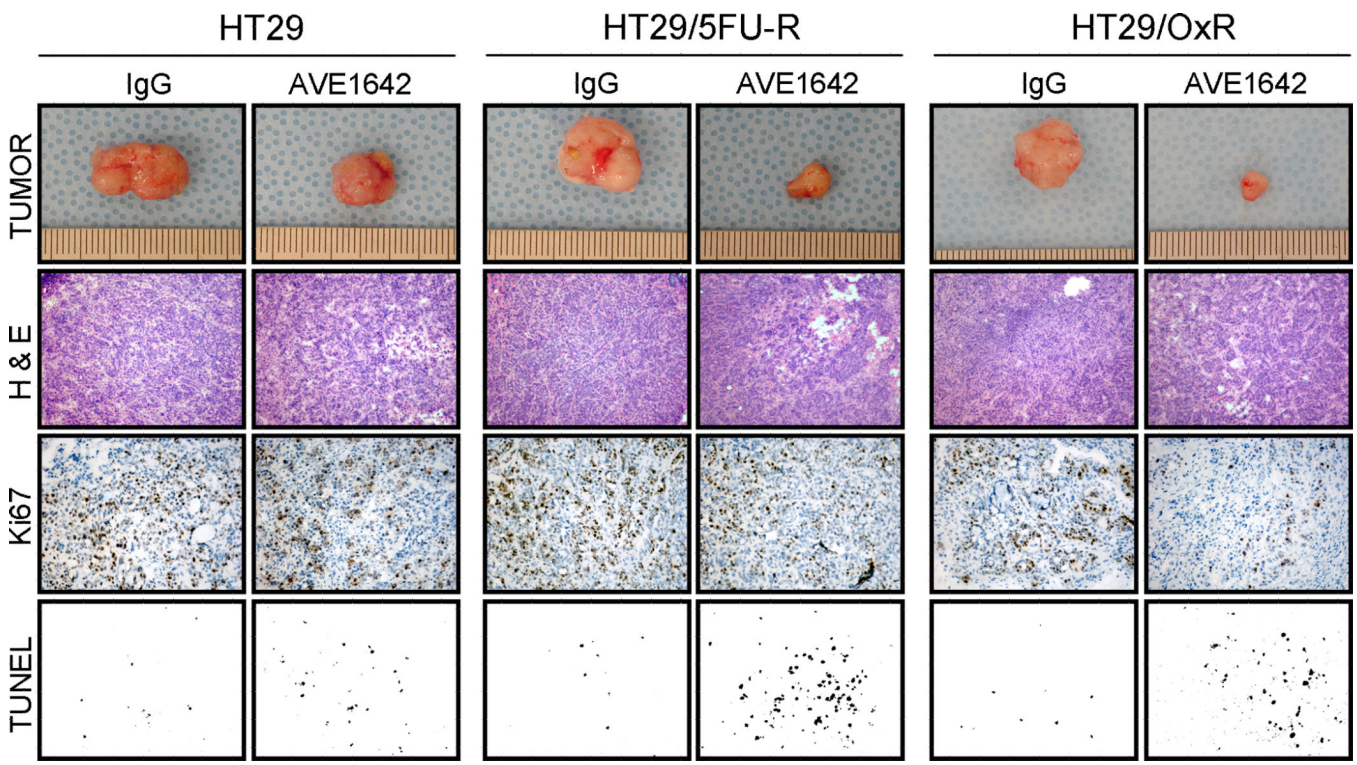

Figure 5. Effect of IGF-1R inhibition on *in vivo* tumor characteristics

Immunohistochemical analysis of tumors was conducted, and multiple tumor fields were evaluated per group. Representative images for all groups from both experiments are presented. H&E staining revealed similar subcutaneous tumor morphology among all groups of tumors. Ki67 staining demonstrated decreased proliferative cells in tumors treated with AVE1642; however, differences in reduction of proliferative cells between parental and resistant-cell-derived tumor sections were not significant. TUNEL staining revealed significantly greater apoptosis in response to AVE1642 in tumors derived from chemoresistant cells than in tumors derived from parental cells ($p<0.05$).